Journal of Chromatography, 175 (1979) 1–20

CHROM. 11,833

IONIC FLUID STRESS EFFECT ON ELECTROOSMOSIS IN ELECTROPHORESIS

T. W. NEE and R. C. HU
Department of Physics, National Central University, Chung-li, Taiwan 320 (Taiwan)
(First received August 3rd, 1978; revised manuscript received January 19th, 1979)

SUMMARY

The electroosmosis effect in electrophoresis experiments has been investigated theoretically using multi-component fluid dynamics. The ionic fluid shearing stress effects and correct boundary conditions have been taken into consideration in order to obtain the solutions of the component fluid velocity profiles. Several model problems with different physical situations and boundary conditions are considered.

INTRODUCTION

The electroosmosis effect is an important phenomenon in electrophoresis experiments[1–4]. Not only the charged mobile ions but also the neutral solvent fluid will move when an electric field is applied along the tube containing the fluid whose components are to be separated. With a long tube with open ends, the fluid will move in one direction; in a tube with closed ends it will circulate[5]. This effect is due to the existence of charge on the tube wall, which induces a double layer in its neighbourhood. When an electric field is applied tangential to the wall surface, there is a net tangential electric force acting on the charged fluid in the double layer, which causes the fluid to move.

A fundamental theory of electroosmosis was presented by Nee[5]. The electrophoretic system is considered as a system of a composite fluid: the neutral solvent fluid and a different ionic charged fluid. These different fluids are described by a set of fluid dynamic equations coupled by the molecular interactions. The set of equations was derived microscopically and applied to a simple model system. The relationship between the double-layer screening length (λ^{-1}), the velocity profiles of different fluid components and the electroosmotic pressure was derived. It was shown that the Poiseulle type of electroosmotic flow is a good approximation to the observations in real electrophoresis experiments.

In the model calculation in ref. 5, the ionic-fluid shearing stress is neglected for mathematical simplification. The ionic flow velocity will always have the form

$$v_{\pm}(y) = v_0(y) \pm \mu_{\pm}^{(0)} E \tag{1}$$

where $v_\pm$ and v_0 are the velocity profiles across the tube and $\mu_\pm^{(0)}$ are the ionic mobilities, E is the electric field along the tube and y is the coordinate on the tube cross-section. Then there are no special boundary conditions for the calculation of $v_\pm(y)$ and, with a closed-ended tube case, $v_\pm(y)$ will never satisfy the mass conservation boundary condition,

$$\int_{-L}^{L} v_\pm(y)\,dy = 0 \tag{2}$$

In addition, with a rough-walled tube, the boundary condition

$$v_\pm(\pm L) = 0 \tag{3}$$

is never satisfied. It is then obvious that the solutions obtained by neglecting the ionic shearing stress are not exact.

In this paper, we present a formal theory with the ionic-fluid shearing stress effect considered. The velocity profiles of different component fluids are calculated. For simple calculation, we chose the same model and geometry of the system as those used earlier[5], which helps us to understand not only the detailed fluid behaviours but also how the solution will reduce to the result in ref. 5 in certain limiting situations.

The general theory is presented in the next section. The multi-component viscous fluid dynamic equation is solved in order to obtain a general solution. The velocity profiles for different physical situations are calculated and discussed in later sections.

GENERAL THEORY

We consider a solution system with A^+, B^- and solvent molecules C^0 in an electric field $\vec{E}$. There are three kinds of fluids, which are described by the density function $n_\alpha(\vec{r}, t)$ and fluid velocity $\vec{v}_\alpha(\vec{r}, t)$ ($\alpha = +, -, 0$ for A^+, B^- and C^0, respectively). They satisfy the equation of continuity

$$\frac{\partial}{\partial t} n_\alpha(\vec{r}, t) + \nabla \cdot [n_\alpha(\vec{r}, t)\,\vec{v}_\alpha(\vec{r}, t)] = 0 \tag{4}$$

and the equation of motion

$$m_\alpha n_\alpha \left[\frac{\partial}{\partial t} + \vec{v}_\alpha \cdot \nabla\right] v_\alpha(\vec{r}, t) = q_\alpha n_\alpha \vec{E} - \sum_{\beta \neq \alpha} \xi_{\alpha\beta} n_\alpha n_\beta (\vec{v}_\alpha - \vec{v}_\beta) - \nabla P_\alpha + \eta_\alpha \nabla^2 \vec{v}_\alpha + \left(v_\alpha + \frac{1}{3}\eta_\alpha\right) \nabla (\nabla \cdot \vec{v}_\alpha) \tag{5}$$

where the terms on the right-hand side are the force densities on the fluid of type α due to different sources: $q_\alpha n_\alpha \vec{E}$ is the electric force density, $-\xi_{\alpha\beta} n_\alpha n_\beta (\vec{v}_\alpha - \vec{v}_\beta)$ the frictional force due to fluid of type β and the last three terms are the self-stress forces. P_α is the partial pressure of component fluid α.

For a simple demonstration of the electroosmosis effect, we consider a cell system bounded by two planes at $y = \pm L$. The external electric field $\vec{E} = [E, 0, 0]$ is applied in the x-direction. We assume that the length Δx and width Δz of the cell are so large that we can neglect edge effects, *i.e.*, we consider the fluid behaviour at a position far from the two edges. In the steady state, the velocities are in the x-direction and will have spatial y-variation only:

$$\vec{v}_\alpha = [v_\alpha(y), 0, 0] \qquad (\alpha = +, -, 0) \tag{6}$$

Then eqn. 5 has the equilibrium form

$$q_\alpha n_\alpha \vec{E} - \sum_{\beta \neq \alpha} \xi_{\alpha\beta} n_\alpha n_\beta (\vec{v}_\alpha - \vec{v}_\beta) - \nabla P_\alpha + \eta_\alpha \nabla^2 v_\alpha = 0 \tag{7}$$

In the presence of the electroosmosis effect, it is assumed that charges exist on the walls of the system. Owing to the electric attraction and repulsion between ions A^+, B^- and the walls, the ionic charges are redistributed in the neighbourhood of the wall and form a double layer there. In our model, the equilibrium densities have the form

$$n_\pm = n_\pm(y) \tag{8}$$

and if we neglect the electric interactions between the charged walls and the neutral solvent molecules (for instance, the electric dipole–quadrupole interactions) we have

$$n_0 = \text{constant} \tag{9}$$

and the electric charge spatial distribution

$$\varrho_e(y) = e[n_+(y) - n_-(y)] \tag{10}$$

by assuming that the electric charges of A^+ and B^- are $+e$ and $-e$, respectively. Following the earlier discussion[5] we finally have the x-component equations

$$\{\pm eE - \xi_\pm n_0 [v_\pm(y) - v_0(y)]\} n_\pm(y) + \eta_\pm v_\pm''(y) - P_{x\pm} = 0 \tag{11}$$

$$\{\xi_+ n_+ [v_+(y) - v_0(y)] + \xi_- n_- [v_-(y) - v_0(y)]\} n_0 + \eta_0 v_0''(y) - P_{x0} = 0 \tag{12}$$

and the y-component equations

$$\mp e\varphi'(y) n_\pm(y) - k_B T n_\pm'(y) = 0 \tag{13}$$

$$-\frac{\partial P_0}{\partial y} = 0 \tag{14}$$

where

$$P_{x\alpha} = \frac{\partial P_\alpha}{\partial x} \tag{15}$$

is the pressure gradient of the component, $q(y)$ is the screening potential due to the double layer ionic charge, and satisfies the Poissons equation

$$\varphi''(y) = -4\pi \varrho_e(y)/\varepsilon \tag{16}$$

and ε is the dielectric constant of the solvent fluid.

Eqn. 13 can be solved to give

$$n_\pm(y) = n_c \, e^{\mp \frac{e}{k_B T} \cdot q(y)} \tag{17}$$

For a high temperature limit, $\frac{eq(y)}{k_B T} \ll 1$,

$$n_\pm(y) \approx n_c \left[1 \mp \frac{e}{k_B T} \cdot \varphi(y)\right] \tag{18}$$

and

$$\varrho_e(y) \approx \frac{2n_c e^2}{k_B T} \cdot \varphi(y) \tag{19}$$

Then the Poisson equation (eqn. 16) can be solved to give

$$\varphi(y) = \varphi_L \cdot \frac{\cos \lambda_s y}{\cos \lambda_s L} \tag{20}$$

where

$$\lambda_s = \sqrt{8\pi n_c e^2/\varepsilon k_B T} \tag{21}$$

λ_s^{-1} is the Debye screening length of the charged fluid. $\varphi_L = \varphi(L)$, the potential at the wall of the cell, and $|\varphi_L|$ is called the zeta potential of the wall. φ_L is negative if we assume that the wall charges are negative (see Fig. 2 in ref. 5).

For mathematical convenience, we define the composite-fluid velocity

$$V(y) = v_0(y) + \frac{\eta_+}{\eta_0} \cdot v_+(y) + \frac{\eta_-}{\eta_0} v_-(y) \tag{22}$$

and the component relative ionic fluid velocity

$$f_\pm(y) = v_\pm(y) - v_0(y) \tag{23}$$

Then the fundamental equations of motion (eqns. 11 and 12) can be transformed into the equations of motion for V and $f_\pm$:

$$V''(y) = \frac{1}{\eta_0}[P_x - E\varrho_e(y)] \tag{24}$$

$$f_\pm''(y) = \mp eE \cdot \frac{n_\pm}{\eta_\pm} + n_0 \left[\xi_\pm n_\pm \left(\frac{1}{\eta_\pm} + \frac{1}{\eta_0}\right) f_\pm(y) + \frac{\xi_\mp n_\mp}{\eta_0} \cdot f_\pm(y)\right] + \frac{P_{x\pm}}{\eta_\pm} - \frac{P_{x0}}{\eta_0} \tag{25}$$

where

$$P_x = P_{x0} + P_{x+} + P_{x-} = \frac{\partial}{\partial x}[P_0 + P_+ + P_-] \tag{26}$$

is the total pressure gradient along the tube.

The mathematics of solving eqns. 24 and 25 are given in the Appendix. The general solutions are

$$\tilde{V}(\tilde{y}) = \frac{P_x L^2}{2\eta_0 v_s} \cdot \tilde{y}^2 - \frac{\cosh(\lambda_s L\tilde{y})}{\cosh(\lambda_s L)} + C \tag{27}$$

$$\tilde{f}(\tilde{y}) = \begin{pmatrix} \tilde{f}_+(\tilde{y}) \\ \tilde{f}_-(\tilde{y}) \end{pmatrix} = -Q^{-1} \cdot R + U \begin{pmatrix} \cosh \varepsilon_+ \tilde{y} & 0 \\ 0 & \cosh \varepsilon_- \tilde{y} \end{pmatrix} \begin{pmatrix} A_+ \\ A_- \end{pmatrix} \tag{28}$$

where

$\tilde{y} = y/L, (-1 \leqslant \tilde{y} \leqslant 1)$

$\tilde{V}(\tilde{y}) = V(y)/v_s$

$\tilde{f}_\pm(\tilde{y}) = f_\pm(y)/v_s$

$v_s = \dfrac{1}{\eta_0} \cdot \dfrac{\varrho_L E}{\lambda_s^2}$

$\varrho_L = \dfrac{2n_c e^2(-q_L)}{k_B T}$ is the fluid charge at the walls

$Q^{-1} = U \cdot \begin{pmatrix} 1/\varepsilon_+^2 & 0 \\ 0 & 1/\varepsilon_-^2 \end{pmatrix} \cdot U^{-1}$

$U = \begin{pmatrix} \varepsilon_+^2 - Q_- & S_- \\ S_+ & -\varepsilon_+^2 + Q_- \end{pmatrix}$

$\varepsilon_\pm^2 = \dfrac{1}{2}[Q_+ + Q_- \pm \sqrt{(Q_+ - Q_-)^2 + 4S_+S_-}]$

$R = \dfrac{L^2}{v_s} \begin{pmatrix} \dfrac{1}{\eta_+} \cdot p_{x+} - \dfrac{1}{\eta_0} \cdot p_{x0} - \dfrac{eEn_c}{\eta_+} \\ \dfrac{1}{\eta_-} \cdot p_{x-} - \dfrac{1}{\eta_0} \cdot p_{x0} + \dfrac{eEn_c}{\eta_-} \end{pmatrix}$

$Q_\pm = \left(1 + \dfrac{\eta_0}{\eta_\pm}\right) S_\pm$

$S_\pm = n_0 n_c \cdot \dfrac{\xi_\pm}{\eta_0} \cdot L^2$

$P_{x\pm}$, P_{x0}, A_+, A_- and C are constants to be determined by suitable boundary conditions. We shall use these results to discuss several special experiments in the following sections.

ELECTROOSMOSIS EFFECT IN AN OPEN-ENDED TUBE WITH ROUGH WALLS

From the definitions in eqns. 22 and 23, the velocity properties of three component fluids are

$$v_0(y) = \frac{V(y) - \frac{\eta_+}{\eta_0} \cdot f_+(y) - \frac{\eta_-}{\eta_0} \cdot f_-(y)}{1 + \eta_+/\eta_0 + \eta_-/\eta_0} \tag{29}$$

and

$$v_\pm(y) = \frac{V(y) + (1 + \eta_\mp/\eta_0) f_\pm(y) - (\eta_\mp/\eta_0) f_\mp(y)}{1 + \eta_+/\eta_0 + \eta_-/\eta_0} \tag{30}$$

Because the two ends are open the pressures at the two ends are equal to the external atmospheric pressure. In addition, because of the geometry symmetry, the partial pressure gradients are vanishing, *i.e.*,

$$P_{x\pm} = P_{x0} = 0 \tag{31}$$

From the rough-walled boundary condition

$$v_0(L) = v_\pm(L) = 0 \tag{32}$$

we have

$$\tilde{V}(1) = \tilde{f}_+(1) = \tilde{f}_-(1) = 0$$

Then the constants C, A_+ and A_- are determined, and we obtain the solution

$$\tilde{V}(\tilde{y}) = 1 - \frac{\cosh(\lambda_s L \tilde{y})}{\cosh(\lambda_s L)} \tag{33}$$

$$\tilde{f}(\tilde{y}) = \left[\mathbf{1} - \boldsymbol{U}\begin{pmatrix} \cosh \varepsilon_+ \tilde{y}/\cosh \varepsilon_+ & 0 \\ 0 & \cosh \varepsilon_- \tilde{y}/\cosh \varepsilon_- \end{pmatrix}\boldsymbol{U}^{-1}\right] \cdot \begin{pmatrix} \mu_+^{(0)} E/v_s \\ -\mu_-^{(0)} E/v_s \end{pmatrix} \tag{34}$$

where

$$\mu_\pm^{(0)} = e/n_0 \xi_\pm \tag{35}$$

are the electric mobilities of the two ions A^+ and B^-.

Substituting eqns. 33 and 34 into eqns. 29 and 30, we can calculate the velocity profiles of the three component fluids. For numerical calculations, we choose $\mu_\pm^{(0)} E = v_s/2$, *i.e.*, $\mu_\pm^{(0)} = \mu_s/2$, and $\eta_+ = \eta_- = 0.01\ \eta_0$. The behaviours for different values of $\lambda_s L$ are shown in Fig. 1. We find that the neutral fluid velocities $v_0(y)$ are approximately the same as that when the ionic shearing stress is neglected ($\eta_+ = \eta_- = 0$) (Fig. 3 in ref. 5). However, the ionic fluid velocities $v_\pm(y)$ are different. This shows that the apparent ionic electric mobilities defined by

$$\mu_\pm(y) = \pm v_\pm(y)/E \tag{36}$$

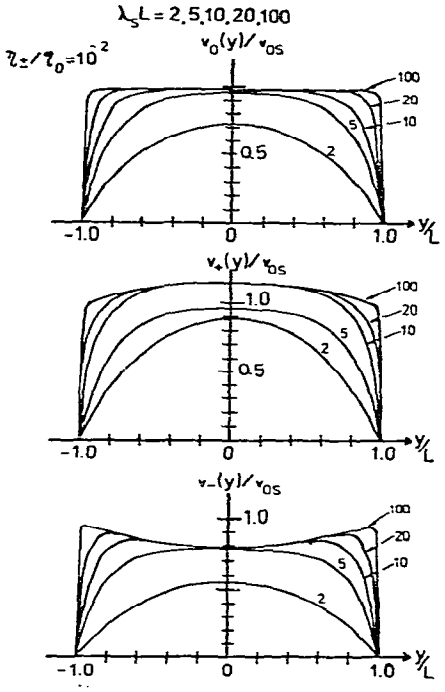

Fig. 1. Electroosmosis effect in an open-ended tube with rough walls. Velocity profiles of component fluids, positive and negative ion flow and neutral solvent flow. Results with different values of the screening parameter $\lambda_s L$ (2, 5, 10 and 100) are shown.

is different from the result (eqn. 43 in ref. 5) obtained by neglecting the ionic shearing stress effect. For quantitative comparisons, choosing $\lambda_s L = 10$, we make numerical calculations for different values of the ionic shearing viscosity: $\eta_\pm/\eta_0 = 10^{-2}$, 10^{-4} and 10^{-6}. The results are shown in Fig. 2. We find that the component fluid will approach the case $\eta_\pm = 0$ (Fig. 3 in ref. 5) in the small $\eta_\pm/\eta_0$ limit. In addition, we find that for $\eta_\pm/\eta_0 \leqslant 10^{-6}$, the fluid will essentially approach the limiting case $\eta_\pm = 0$. The only appreciable difference comes from the double-layer region with thickness λ_s^{-1} about the wall. For a typical electrophoresis system, $\lambda_s^{-1} \approx 10^{-6}$ cm and $\eta_\pm/\eta_0 \approx 10^{-9}$ (ref. 5). Then it is an excellent approximation to neglect the ionic-fluid shearing effect except in the double layer region which is very close to the tube wall. The solvent will move at constant velocity

$$v_0(y) \approx v_{os} = v_s = \frac{1}{\eta_0} \cdot \frac{\varrho_L E}{\lambda_s^2}$$

where v_{os} is the electroosmotic velocity.

ELECTROOSMOSIS EFFECT IN A CLOSED-ENDED TUBE

In a closed-ended tube, the fluid pulled by the electric field E near the wall cannot keep its forward motion everywhere across the tube cross-section. The fluid

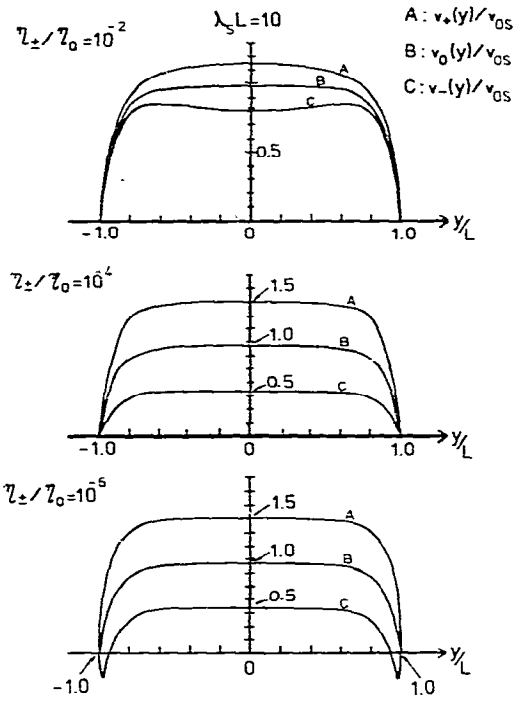

Fig. 2. Ionic-fluid effect of electroosmosis in an open-ended tube with rough walls. Results with $\eta_\pm/\eta_0 = 10^{-2}$, 10^{-4} and 10^{-6} are shown.

will be pushed back by the end-walls and a counter flow is formed at the centre[5]. We assume that the tube is very long, so that we can neglect the end effect when we are considering the fluid far from the ends. Owing to the mass conservation of component fluid at any cross-section, instead of eqn. 31 we have the boundary conditions

$$\int_{-L}^{L} v_0(y)\,dy = 0 \tag{37}$$

for solvent fluid and

$$\int_{-L}^{L} v_\pm(y)\,dy = 0 \tag{38}$$

for ionic fluids.

Another boundary condition is due to the tube-wall condition. We consider two limiting cases: a rough wall and a smooth wall.

The rough-walled cell

If the wall is so rough that all fluids cannot move there, the rough wall boundary condition is

$$v_\alpha(\pm L) = 0 \qquad (\alpha = 0, +, -) \tag{39}$$

From eqns. 27–30 and 37–39, we obtain the solution

$$v_0(y) = v_+(y) = v_-(y) = \frac{V(y)}{1 + \eta_+/\eta_0 + \eta_-/\eta_0} \tag{40}$$

$$\frac{V(y)}{v_s} = \tilde{V}(\tilde{y}) = \frac{3}{2}\left[1 - \frac{\tanh(\lambda_s L)}{\lambda_s L}\right](\tilde{y}^2 - 1) + 1 - \frac{\cosh(\lambda_s L\tilde{y})}{\cosh(\lambda_s L)} \tag{41}$$

and the pressure gradients

$$P_{x0} = \frac{1}{1 + \eta_+/\eta_0 + \eta_-/\eta_0} \cdot \frac{3\varrho_L E}{(\lambda_s L)^2}\left[1 - \frac{\tanh(\lambda_s L)}{\lambda_s L}\right] \tag{42}$$

for neutral solvent fluid and

$$P_{x\pm} = \pm en_c E + \frac{\eta_\pm}{\eta_0} \cdot P_{x0} \tag{43}$$

for ionic fluids. Note that in most practical cases, $\lambda_s L \gg 1$ and $\eta_\pm/\eta_0 \ll 1$ (ref. 5), we have

$$v_0(y) \approx \frac{v_{os}}{2}(3\tilde{y}^2 - 1) \tag{44}$$

where the electroosmotic velocity is

$$v_{os} = v_s = \varrho_L E/\lambda_s^2 \eta_0 \tag{45}$$

By choosing $\eta_+/\eta_0 = \eta_-/\eta_0 = 10^{-2}$, the numerical result is as shown in Fig. 3.

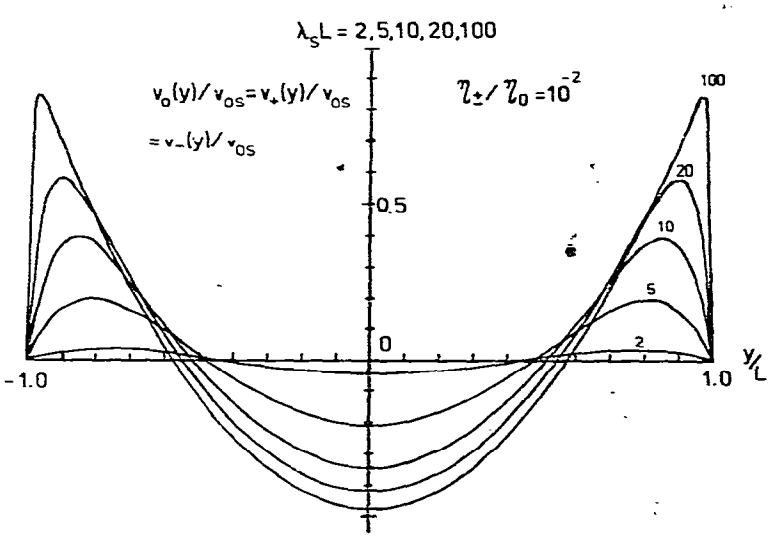

Fig. 3. Electroosmosis effect in a closed-ended tube with rough walls. The velocity profiles of the neutral solvent and ionic fluids are the same. Results with different values of the screening parameter $\lambda_s L$ (2, 5, 10 and 100) are shown. $\eta_\pm/\eta_0 = 10^{-2}$ and $v_{os} = v_s$.

The smooth-walled cell

If the wall is perfectly smooth with respect to the three component fluids, their stress at the wall will vanish, and instead of eqn. 39 we have

$$v_a'(\pm L) = 0 \tag{46}$$

All other boundary conditions are the same as for the rough-walled cell. The results are

$$v_0(y) = v_+(y) = v_-(y) = \frac{V(y)}{1 + \eta_+/\eta_0 + \eta_-/\eta_0} \tag{47}$$

$$\frac{V(y)}{v_s} = \tilde{V}(\tilde{y}) = \frac{\lambda_s L}{2} \cdot \tanh(\lambda_s L)\left(\tilde{y}^2 - \frac{1}{3}\right) + \frac{1}{\lambda_s L} \cdot \tanh(\lambda_s L) - \frac{\cosh(\lambda_s L \tilde{y})}{\cosh(\lambda_s L)} \tag{48}$$

and the pressure gradients are

$$P_{x0} = \frac{1}{1 + \eta_+/\eta_0 + \eta_-/\eta_0} \cdot \frac{\varrho_L E}{\lambda_s L} \cdot \tanh(\lambda_s L) \tag{49}$$

and

$$P_x = \pm eEn_c + \frac{\eta_\pm}{\eta_0} \cdot p_{x0} \tag{50}$$

In practical cases, $\lambda_s L \gg 1$ and $\eta_\pm/\eta_0 \ll 1$. At locations not very near to the tube walls, $v_0(y) \approx (v_{os}/2)(3\tilde{y}^2 - 1)$ with the electroosmotic velocity $v_{os} = v_0 \cdot \lambda_s L/3$. By choosing $\eta_\pm/\eta_0 = 10^{-2}$, the numerical results are as shown in Fig. 4.

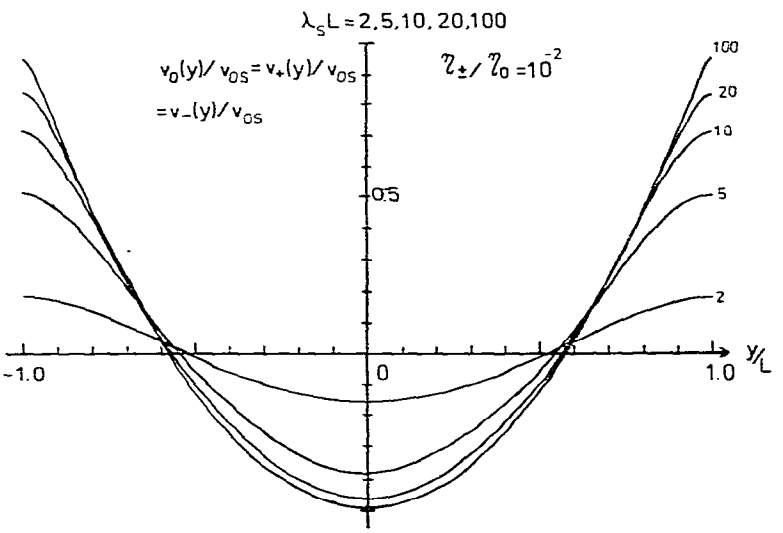

Fig. 4. Electroosmosis effect in a closed-ended tube with smooth walls. The parameters chosen are $\eta_\pm/\eta_0 = 10^{-2}$, $\lambda_s L = 2$, 5, 10 and 100 and $v_{os} = v_s \lambda_s L/3$.

Comparing Figs. 3 and 4 in this paper with Figs. 4 and 5 in ref. 5, respectively, we find that the neutral solvent fluid has the same velocity profile shape except for a reduction in magnitude by a factor $(1 + \eta_+/\eta_0 + \eta_-/\eta_0)$. However, the ionic fluid motions are different: their velocity profiles in Figs. 4 and 5 in ref. 5 are wrong: the ionic fluid should move together with the solvent fluid.

The pressure gradient results in eqns. 42, 43, 49 and 50 can be understood as follows. When the tube is closed, the end walls will make a counter pressure to balance the electric force ($\mp e E n_c$) and an additional mechanical force ($\eta_\pm/\eta_0 \cdot P_{x0}$) to push back the ionic fluid. For a neutral solvent fluid, only mechanical force P_{x0} is necessary.

PRACTICAL SYSTEMS

Electrophoresis is a special technique for separating the charged component fluids according to their different mobilities. Usually, the mixture of ions to be separated occupies a small portion in a long electrophoresis tube. In a practical situation, the closed-ended boundary condition in eqn. 38 for ionic fluids is not satisfied, despite the fact that the tube is closed, and eqn. 37 for the neutral solvent fluid is always satisfied. In this situation, eqn. 38 should be replaced with

$$P_{x\pm} = 0 \tag{51}$$

i.e., the ionic fluids cannot "see" the closed ends because they are far away.

We discuss the characteristics in three cases below.

Rough-walled cell

As the first example, we consider the case of a rough walled cell. The component fluid profiles v_0 and $v_\pm$ are given by eqns. 29 and 30, and

$$\tilde{V}(\tilde{y}) = \frac{P_x L^2}{\eta_0 v_s}\left[\frac{\tilde{y}^2 - 1}{2}\right] + 1 - \frac{\cosh(\lambda_s L\tilde{y})}{\cosh(\lambda_s L)} \tag{52}$$

$$\tilde{f}(\tilde{y}) = \left[1 - \boldsymbol{U}\begin{pmatrix}\cosh\varepsilon_+\tilde{y}/\cosh\varepsilon_+ & 0\\ 0 & \cosh\varepsilon_-\tilde{y}/\cosh\varepsilon_-\end{pmatrix}\boldsymbol{U}^{-1}\right]\times$$

$$\times\begin{pmatrix}\mu_+^{(0)}E/v_s\\ -\mu_-^{(0)}E/v_s\end{pmatrix} + \frac{p_x L^2}{\eta_0 v_s}\cdot\boldsymbol{Q}^{-1}\begin{pmatrix}1\\1\end{pmatrix} \tag{53}$$

where

$$\frac{P_x L^2}{\eta_0 v_s} = 3\,[1 - \tanh(\lambda_s L)/(\lambda_s L) - \beta]/(1 + 3\gamma) \tag{54}$$

$$\beta = \left(\frac{\eta_+}{\eta_0}, \frac{\eta_-}{\eta_0}\right)\left[\mathbf{1} - \boldsymbol{U}\begin{pmatrix}\tanh\varepsilon_+/\varepsilon_+ & 0\\ 0 & \tanh\varepsilon_-/\varepsilon_-\end{pmatrix}\right]\boldsymbol{U}^{-1}\begin{pmatrix}\mu_+^{(0)}E\\ -\mu_-^{(0)}E\end{pmatrix} \tag{55}$$

$$\gamma = \left(\frac{\eta_+}{\eta_0}, \frac{\eta_-}{\eta_0}\right)\left[\mathbf{1} - \boldsymbol{U}\begin{pmatrix}\tanh\varepsilon_+/\varepsilon_+ & 0\\ 0 & \tanh\varepsilon_-/\varepsilon_-\end{pmatrix}\boldsymbol{U}^{-1}\right]\boldsymbol{Q}^{-1}\begin{pmatrix}1\\1\end{pmatrix} \tag{56}$$

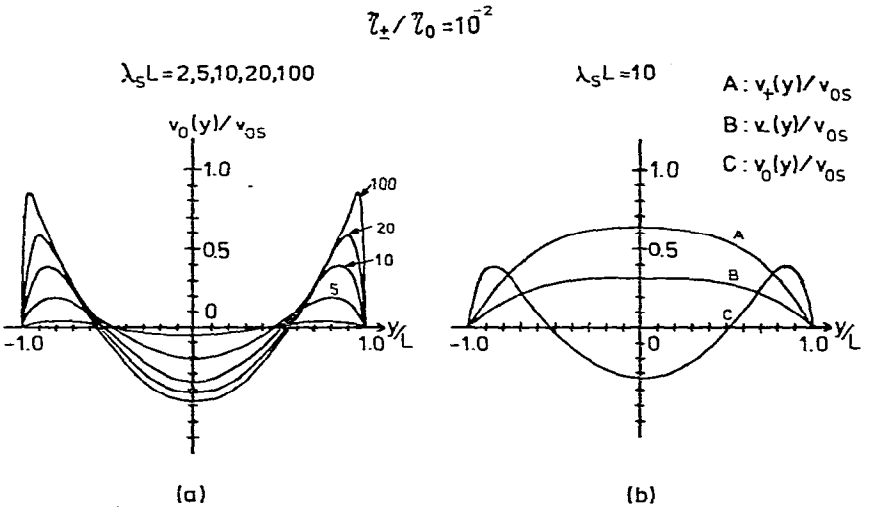

Fig. 5. Electroosmosis effect in a long closed-ended tube with rough walls. Ionic fluids occupy finite space and cannot "see" the closed ends. $\eta_\pm/\eta_0 = 10^{-2}$. (a) Neutral solvent fluid profiles; (b) three component fluid profiles for $\lambda_s L = 10$.

By choosing $\eta_\pm/\eta_0 = 10^{-2}$, the characteristic behaviours are as shown in Fig. 5. We find that the neutral fluid profiles (Fig. 5a) are approximately the same as that obtained by neglecting the ionic shearing stress (Fig. 4b in ref. 5). The ionic fluid profiles are shown in Fig. 5b.

To demonstrate the ionic-shearing effect, we show the results for $\eta_\pm/\eta_0 = 10^{-4}$ and 10^{-6} in Fig. 6. For a larger ionic-shearing stress (larger $\eta_\pm/\eta_0$), the ionic fluids will couple strongly and tend to move together (*i.e.*, the second term in eqn. 53 will

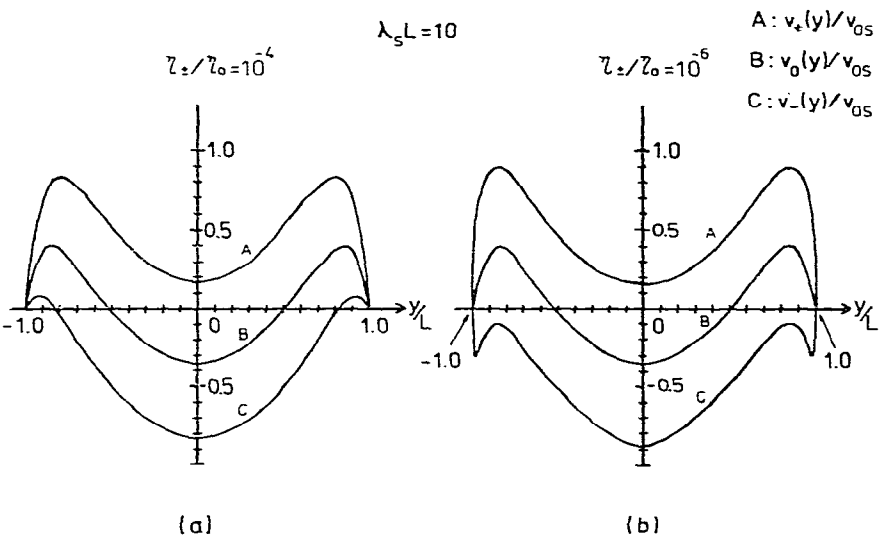

Fig. 6. Ionic-shearing stress effect for the same system as in Fig. 5. $\lambda_s L = 10$. (a) $\eta_\pm/\eta_0 = 10^{-4}$; (b) $\eta_\pm/\eta_0 = 10^{-6}$.

contribute more significantly). We find that Fig. 4a in ref. 5 is essentially the small $\eta_\pm/\eta_0$ limit of this case. This is not related to the rough-walled cell case in the last section.

Smooth-walled cell

We consider next the case of a smooth-walled cell. The results are

$$\tilde{V}(\tilde{y}) = \frac{1}{2} \cdot \frac{P_x L^2}{\eta_0 v_s} \left(\tilde{y}^2 - \frac{1}{3}\right) + \frac{\tanh(\lambda_s L)}{\lambda_s L} - \frac{\cosh(\lambda_s L \tilde{y})}{\cosh(\lambda_s L)} + \\ + \left(\frac{\eta_+}{\eta_0}, \frac{\eta_-}{\eta_0}\right) \boldsymbol{W} \tag{57}$$

and

$$\tilde{f}(\tilde{y}) = \boldsymbol{W} = \frac{P_x L^2}{\eta_0 v_s} \cdot \boldsymbol{Q}^{-1} \begin{pmatrix} 1 \\ 1 \end{pmatrix} + \begin{pmatrix} \mu_+^{(0)} E/v_s \\ -\mu_-^{(0)} E/v_s \end{pmatrix} \tag{58}$$

where

$$\frac{P_x L^2}{\eta_0 v_s} = \lambda_s L \tanh(\lambda_s L)$$

We find that, at the small $\eta_\pm/\eta_0$ limit, eqn. 57 is identical with eqn. 48; thus the neutral fluid profile $v_0(y)$ is not affected by the open-ended boundary condition of $v_\pm(y)$. However, $f_\pm = v_\pm - v_0$ are non-zero constants. Then the charged fluids will move differently from the neutral solvent fluid owing to the open end. Choosing $\eta_\pm/\eta_0 = 10^{-2}$, the characteristic behaviours are as shown in Fig. 7. To demonstrate the ionic-shearing stress effect, for $\lambda_s L = 10$, the results for $\eta_\pm/\eta_0 = 10^{-4}$ and 10^{-6}

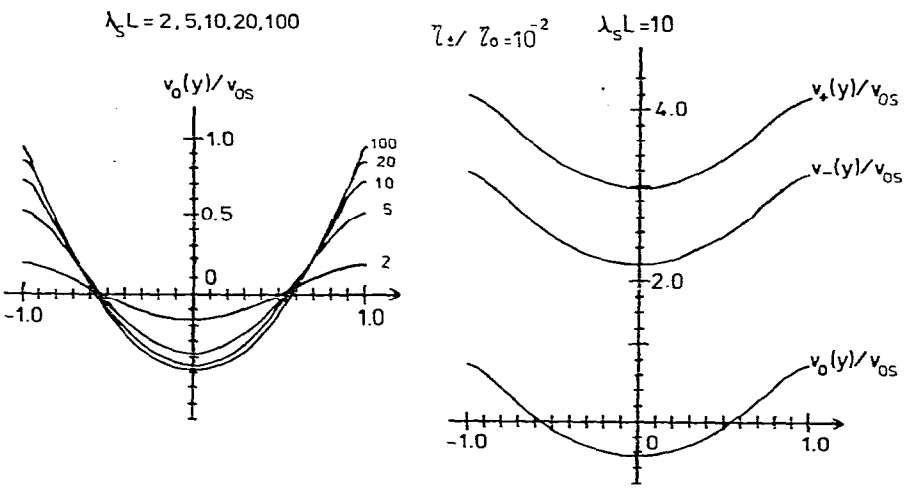

Fig. 7. Electroosmosis effect in a long closed-ended tube with smooth walls. Ionic fluids occupy a finite region and cannot "see" the closed ends. $\eta_\pm/\eta_0 = 10^{-2}$. (a) Neutral solvent fluid profiles; (b) three component fluid profiles for $\lambda_s L = 10$.

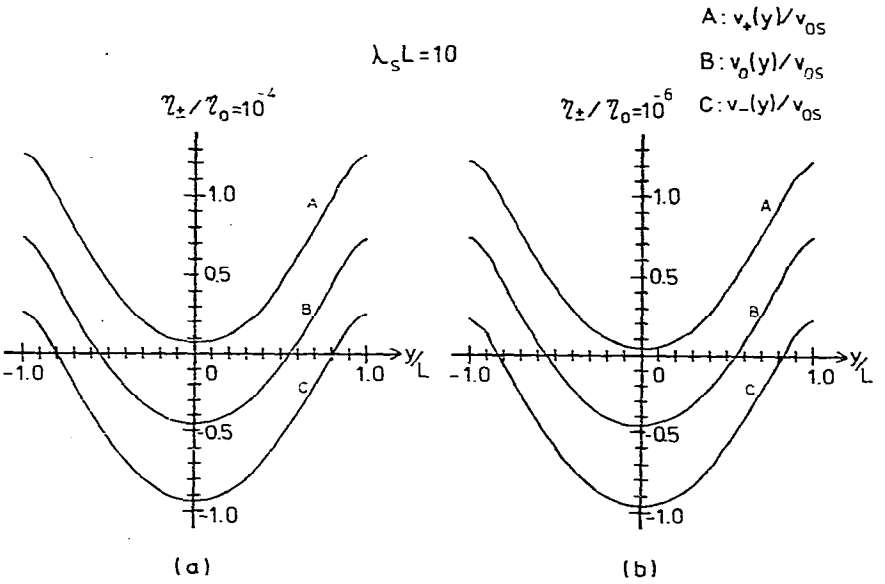

Fig. 8. Ionic-shearing stress effect for the same system as in Fig. 7.

are shown in Fig. 8. For a larger ionic-shearing stress (larger $\eta_\pm/\eta_0$), the ionic fluids will couple strongly and tend to move together. The first term of eqn. 58 will contribute more significantly. We find that Fig. 5a in ref. 5 is essentially the small $\eta_\pm/\eta_0$ limit of this case. This is not related to the smooth-walled cell case in the last section.

Mixed case

In addition, the ionic concentrations are usually so small that the frictional forces between the walls and the ionic fluid may be small in comparison with that of neutral solvent fluid. Therefore, it would be interesting to study the case when the wall will be smooth towards ionic fluids but rough to the neutral solvent fluid, *i.e.*, the boundary conditions are

$$v_0(\pm L) = 0$$

and

$$v_\pm'(\pm L) = 0$$

Then the results are

$$\tilde{V}(\tilde{y}) = \frac{1}{2} \cdot \frac{P_x L^2}{\eta_0 v_s} \cdot \tilde{y}^2 - \frac{\cosh(\lambda_s L \tilde{y})}{\cosh(\lambda_s L)} + C \tag{59}$$

$$\tilde{f}(\tilde{y}) = W + \left(\lambda_s L \tanh \lambda_s L - \frac{P_x L^2}{\eta_0 v_s}\right) \times$$

$$\times U \begin{pmatrix} \cosh \varepsilon_+ \tilde{y}/\varepsilon_+ \sinh \varepsilon_+ & 0 \\ 0 & \cosh \varepsilon_- \tilde{y}/\varepsilon_- \sinh \varepsilon_- \end{pmatrix} U^{-1} \begin{pmatrix} 1 \\ 1 \end{pmatrix} \tag{60}$$

where

$$\frac{P_x L^2}{\eta_0 v_s} = \frac{3\,[1 - \tan(\lambda_s L)/(\lambda_s L)] + \gamma \lambda_s L \tanh(\lambda_s L)}{1 + \gamma}$$

$$C = 1 - \frac{1}{2} \cdot \frac{P_x L^2}{\eta_0 v_s} + \alpha \left(\lambda_s L \tanh \lambda_s L - \frac{P_x L^2}{\eta_0 v_s}\right) + \left(\frac{\eta_+}{\eta_0}, \frac{\eta_-}{\eta_0}\right) W \tag{62}$$

$$W = \frac{P_x L^2}{\eta_0 v_s} \cdot Q^{-1} \begin{pmatrix} 1 \\ 1 \end{pmatrix} + \begin{pmatrix} \mu_+^{(0)} E/v_s \\ -\mu_-^{(0)} E/v_s \end{pmatrix} \tag{63}$$

$$\gamma = 3(\alpha - \beta) \tag{64}$$

$$\alpha = \left(\frac{\eta_+}{\eta_0}, \frac{\eta_-}{\eta_0}\right) U \begin{pmatrix} \operatorname{ctnh} \varepsilon_+/\varepsilon_+ & 0 \\ 0 & \operatorname{ctnh} \varepsilon_-/\varepsilon_- \end{pmatrix} U^{-1} \begin{pmatrix} 1 \\ 1 \end{pmatrix} \tag{65}$$

$$\beta = \left(\frac{\eta_+}{\eta_0}, \frac{\eta_-}{\eta_0}\right) U \begin{pmatrix} 1/\varepsilon_+^2 & 0 \\ 0 & 1/\varepsilon_-^2 \end{pmatrix} U^{-1} \begin{pmatrix} 1 \\ 1 \end{pmatrix} \tag{66}$$

It can be calculated that the electroosmotic velocity v_{os} is v_s, the same as the case for rough-walled and closed-ended tubes.

By choosing $\eta_\pm/\eta_0 = 10^{-2}$, the fluid profiles are as shown in Fig. 9. Because the wall is smooth, the ionic fluids are strongly coupled and nearly move together.

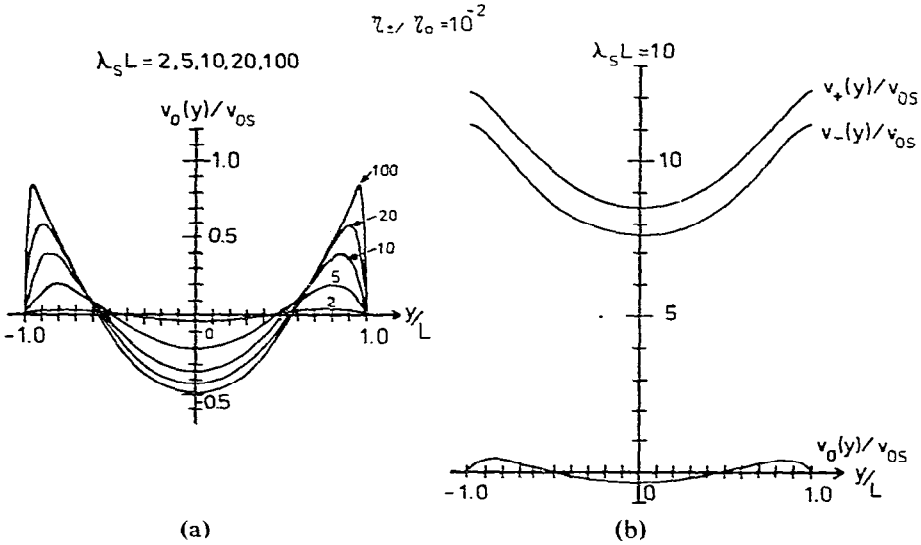

(a) (b)

Fig. 9. Electroosmosis effect in a long closed-ended tube with walls rough to neutral solvent fluid and smooth to ionic fluids. Ionic fluids occupy a finite region and cannot "see" the closed ends. $\eta_\pm/\eta_0 = 10^{-2}$. (a) Neutral solvent fluid profiles; (b) three component fluid profiles for $\lambda_s L = 10$.

The ionic-shearing stress effect is shown in Fig. 10. We find that Fig. 4a in ref. 5 is also the small $\eta_\pm/\eta_0$ limit of this case.

We find that the higher value of λ_s, the larger is the electric force which causes the electroosmotic effect and then the higher are the ionic fluid velocities. Because we assume no frictional force between the walls and the fluids, also there is no counter

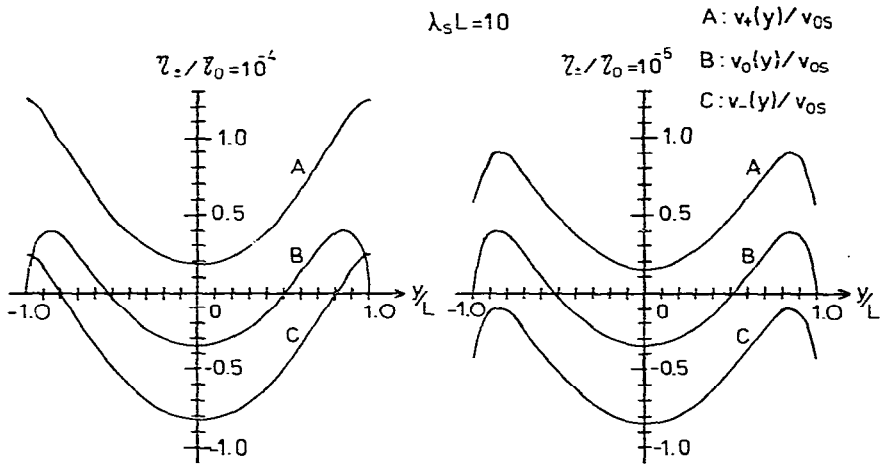

Fig. 10. Ionic-fluid effect for the same system as in Fig. 9.

pressure to push the ionic fluid back, and then the ionic fluid velocities increase very rapidly as λ_s increases, *i.e.*, the electric force due to the double layer becomes larger. This is snown in Fig. 11. Then the closed-ended tube with the rough-walled case in ref. 5 is not the limiting case of this calculation.

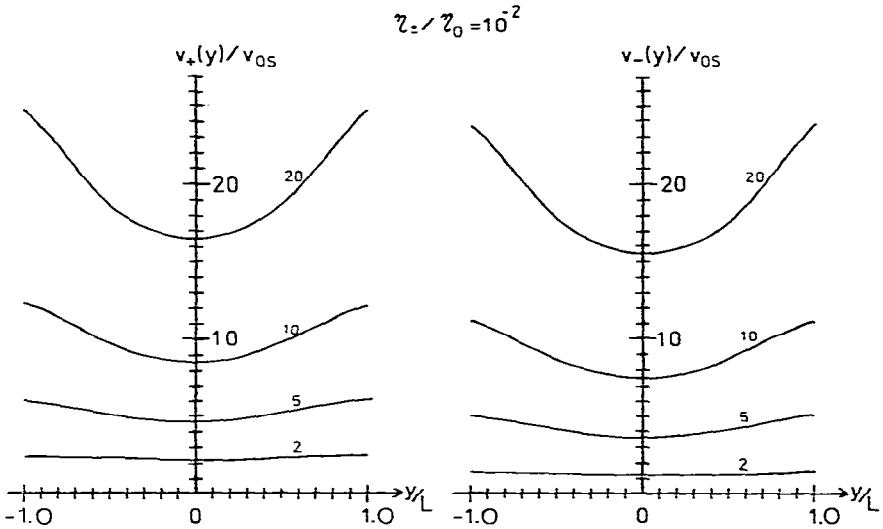

Fig. 11. Double-layer effect for the same system as in Fig. 9.

DISCUSSION

We have formally solved the problem of electroosmosis with the consideration of ionic-fluid shearing stress, which was neglected in a previous paper[5]. The ionic-fluid profiles $v_{\pm}$ have been calculated with corrected boundary conditions. The exact solutions are obtained by means of eigenvalue formulism in matrix form (see Appendix).

We have considered six cases with different boundary conditions:

(i) open-ended tube, rough walls to all three component fluids;

(ii) closed-ended tube, rough walls to all three component fluids;

(iii) closed-ended tube, smooth walls to all three component fluids;

(iv) closed-ended tube, rough walls to the neutral solvent fluid, but open ended with rough walls to both ionic fluids;

(v) closed-ended tube, smooth walls to neutral solvent fluid, but open-ended with smooth walls to both ionic fluids;

(vi) closed-end tube, rough wall to solvent fluid, but open-ended with smooth walls to both ionic fluids.

In the limit $\lambda_s L \to \infty$, $\eta_\pm/\eta_0 \to 0$, cases (i), (iv) and (v) will approach to the results in ref. 5 except at the double-layer region near the wall. This is correct because, in ref. 5, the boundary condition of ionic fluids at the wall was neglected and an incorrect solution was obtained. By including the ionic-shearing stress effect and the corrected boundary condition for ionic fluid, we obtain consistent results in the double-layer region near the wall.

In order to obtain an analytical solution, we have made the approximation

$$n_\pm \approx n_c \tag{67}$$

in the calculation of $f_\pm = v_\pm - v_0$. This is a good approximation except inside the double layer near the wall (see Fig. 2a in ref. 5). In practice, as the double-layer region is very small, we expect that this would be a good approximation. However, this effect can be calculated by means of a perturbation approach. It is expected that the profile will be distorted in the double-layer region and does not change the fundamental characteristics appreciably.

It is interesting to study this ionic fluid effect experimentally. Up to now, only the solvent fluid motion has been observed[1,4]. Component fluid motion has never been observed or studied experimentally. One possible situation is that similar to the case of a closed-ended tube with rough walls where all component fluids move together. However, other cases are also possible. Hence it is one purpose of this paper to draw attention to the need to design suitable experiments in order to observe the ionic fluid effects. Possibly some solutions with different ions of different colours will be suitable for the experimental system.

Because of the friction between component fluids, Joule heat would be generated, associated with the electric currents due to the moving charged fluids. This effect will cause temperature inhomogeneities across the tube cross-section. The assumption of homogeneous temperature in this paper therefore should be modified, and this aspect will be discussed in subsequent papers.

APPENDIX

Mathematics of solving the component fluid equations

To obtain $V(y)$, we substitute eqns. 19 and 20 into eqn. 24, and solve by simple integration:

$$V(y) = \frac{P_x}{2\eta_0} \cdot y^2 - v_s \cdot \frac{\cosh(\lambda_s y)}{\cosh(\lambda_s L)} + C' \tag{A-1}$$

where

$$v_s = \frac{1}{\eta_0} \cdot \frac{\varrho_L L}{\lambda_s^2} \tag{A-2}$$

and

$$\varrho_L = \frac{2n_c e^2}{k_B T} \cdot q_L \tag{A-3}$$

is the charge concentration at the tube centre ($y = 0$). Here we have used geometric symmetry: $V(y)$ and $f_\pm(y)$ are even functions of y.

For mathematical simplification, we define the dimensionless quantities

$$\tilde{V}(\tilde{y}) = V(y)/v_s \tag{A-4}$$

$$\tilde{f}_\pm(\tilde{y}) = f_\pm(y)/v_s \tag{A-5}$$

and

$$\tilde{y} = y/L \qquad (|\tilde{y}| \leqslant 1) \tag{A-6}$$

where

$$v_s = \frac{\varrho_L E}{\eta_0 \lambda_s^2} \tag{A-7}$$

Then the solution A–1 can be rewritten as

$$\tilde{V}(\tilde{y}) = \frac{P_x L^2}{2\eta_0 v_s} \cdot \tilde{y}^2 - \frac{\cosh(\lambda_s L \tilde{y})}{\cosh(\lambda_s L)} + C \tag{A-8}$$

where C is a constant to be determined by the boundary conditions.

To obtain $f_\pm(y)$, we define the matrix

$$\tilde{\boldsymbol{f}}(\tilde{y}) = \begin{pmatrix} f_+(\tilde{y})/v_s \\ f_-(\tilde{y})/v_s \end{pmatrix} \tag{A-9}$$

In practice, we consider the high temperature limit

$$\left|\frac{eq(y)}{k_B T}\right| \leqslant \frac{e|q_L|}{k_B T} \ll 1 \tag{A-10}$$

For mathematical simplicity, we neglect the spatial variation of ionic concentration in eqn. 18,

$$n_\pm(y) \approx n_c \tag{A-11}$$

and from eqns. 25 and A–9 we have the differential equation for $\tilde{\boldsymbol{f}}(\tilde{y})$:

$$\frac{\mathrm{d}^2}{\mathrm{d}y^2} \cdot \tilde{\boldsymbol{f}}(\tilde{y}) = \boldsymbol{Q}\tilde{\boldsymbol{f}} + \boldsymbol{R} \tag{A-12}$$

where

$$\boldsymbol{Q} = \begin{pmatrix} Q_+ & S_- \\ S_+ & Q_- \end{pmatrix} \tag{A-13}$$

$$\boldsymbol{R} = \begin{pmatrix} P_+ - p_0 - q_+ \\ P_- - p_0 + q_- \end{pmatrix} \frac{L^2}{v_s} \tag{A-14}$$

$$S_\pm = n_0 n_c \xi_\pm L^2/\eta_0 \tag{A-15}$$

$$Q_\pm = \left(\frac{\eta_0}{\eta_\pm} + 1\right) S_\pm \tag{A-16}$$

$$P_\alpha = P_{x\alpha}/\eta_\alpha \quad (\alpha = 0, +, -) \tag{A-17}$$

and

$$q_\pm = e E n_c/\eta_\pm \tag{A-18}$$

To solve eqn. A–12, we first solve the following eigenvalue equation

$$\mathbf{Q}\boldsymbol{\alpha} = \varepsilon^2 \boldsymbol{\alpha} \tag{A-19}$$

We obtain the eigenvalues

$$\varepsilon_\pm{}^2 = \frac{1}{2}[Q_+ + Q_- \pm \sqrt{(Q_+ - Q_-)^2 + 4S_+S_-}] \tag{A-20}$$

and the eigenvectors

$$\boldsymbol{\alpha}_+ = \begin{pmatrix} \varepsilon_+{}^2 - Q_- \\ S_+ \end{pmatrix}; \quad \boldsymbol{\alpha}_- = \begin{pmatrix} S_- \\ -\varepsilon_+{}^2 + Q_- \end{pmatrix} \tag{A-21}$$

Then if we define the matrix

$$\boldsymbol{U} = (\boldsymbol{\alpha}_+, \boldsymbol{\alpha}_-) = \begin{pmatrix} \varepsilon_+{}^2 - Q_- & S_- \\ S_+ & -\varepsilon_+{}^2 + Q_- \end{pmatrix} \tag{A-22}$$

we have

$$\boldsymbol{Q} = \boldsymbol{U} \begin{pmatrix} \varepsilon_+{}^2 & 0 \\ 0 & \varepsilon_-{}^2 \end{pmatrix} \boldsymbol{U}^{-1} \tag{A-23}$$

Then eqn. A–12 can easily be solved, and we obtain the solution

$$\tilde{f}(\tilde{y}) = -\boldsymbol{Q}^{-1}\boldsymbol{R} + \boldsymbol{U} \begin{pmatrix} \cosh \varepsilon_+ \tilde{y} & 0 \\ 0 & \cosh \varepsilon_- \tilde{y} \end{pmatrix} \begin{pmatrix} A_+ \\ A_- \end{pmatrix} \tag{A-24}$$

where A_+ and A_- are constants to be determined by the boundary conditions.

ACKNOWLEDGEMENT

This study was supported in part by the National Research Council, Taiwan.

REFERENCES

1 H. A. Abramson, L. S. Moyer and M. H. Gorin, *Electrophoresis of Proteins and the Chemistry of Cell Surface*, Hafner, New York, 1964, Ch. 1 and 5.
2 C. C. Brinton, Jr., and M. A. Lauffer, in M. Bier (Editor), *Electrophoresis, Theory, Methods and Application*, Vol. 1, Academic Press, New York, 1959, Ch. 10.
3 E. Heftmann, *Chromatography*, Reinhold, New York, 1967, Ch. 10.
4 C. Fan, *Convection Phenomena in Electrophoresis Separation*, LMSC-HREC TR D306 300, Lockheed Missiles and Space Co., Huntsville, Ala., 1972.
5 T. W. Nee, *J. Chromatogr.*, 105 (1975) 231.